Biochimica et Biophysica Acta, 680 (1982) 44–59
Elsevier Biomedical Press

BBA 41064

RADICAL-PAIR DECAY KINETICS, TRIPLET YIELDS AND DELAYED FLUORESCENCE FROM BACTERIAL REACTION CENTERS

CRAIG C. SCHENCK *, ROBERT E. BLANKENSHIP ** and WILLIAM W. PARSON

Department of Biochemistry, University of Washington, Seattle, WA 98195 (U.S.A.)

(Received August 18th, 1981)

Key words: Reaction center; Delayed fluorescence; Quantum yield; Photosynthesis; (Rps. sphaeroides, R. rubrum)

Purified reaction centers from *Rhodopseudomonas sphaeroides* and *Rhodospirillum rubrum* were excited with short flashes of light, under conditions that blocked electron transfer to the first quinone (Q). The radical-pair state (P^F) generated by the excitation decays by several different back-reactions. One back-reaction repopulates an excited singlet state (P*) and results in delayed fluorescence; another produces a triplet state (P^R). We measured the decay kinetics of P^F, the quantum yield of P^R, and the intensity and decay kinetics of the delayed fluorescence under a variety of conditions, including cryogenic temperatures, magnetic fields, depletion of Q and Fe, and isotopic replacement of ^1H by ^2H. The delayed fluorescence decays about twice as rapidly as P^F, and has an unusual temperature dependence. It increases in amplitude with decreasing temperature from 260 to 215 K, and then decreases. From the amplitude of the delayed fluorescence, we estimate the standard free energy and enthalpy differences between P^F and P*, and an effective rate constant for the repopulation of P*, as functions of temperature. Regeneration of P* accounts for only a small fraction of the decay of P^F. Contrary to expectation, the quantum yield of P^R is not decreased by deuteration of the reaction centers, or by depletion of Q or Fe. The known decay paths of P^F cannot fully account for the dependence of the P^R yield and the decay kinetics of P^F on temperature and magnetic fields, nor for the decay kinetics and temperature dependence of the delayed fluorescence. Possible solutions to some of these problems are suggested.

Introduction

In reaction centers of photosynthetic bacteria, oxidation of a bacteriochlorophyll dimer (P) occurs within a few picoseconds after absorption of a photon [1–5]. An electron is transferred to an acceptor complex (I) that includes a bacteriopheophytin (H) and a bacteriochlorophyll (B) [6,7]. This generates a transient radical-pair state (P^+I^- or state P^F). Recent work [8] suggests that P^F is a mixture of at least two states, $^1[P^+B^-]$ and $^1[P^+H^-]$. $^1[P^+B^-]$ is probably formed initially from an excited singlet state of P (P*) [5]. An electron appears on H in about 4 ps [4], and moves from H^- to a quinone (Q) in about 200 ps [2,3]. If Q is reduced before the excitation or is extracted from the reaction centers, P^F lives much longer, decaying in 10–20 ns by several types of back-reaction [8–12]. Under these conditions, one sees a 2- to 3-fold increase in the fluorescence from P [1,13–19], and also the formation of a triplet state (state P^R) [8,10,20–23]. P^R, which has a lifetime of 10–100 μs, appears to be a mixture of an excited

* Present address: CENS, Service de Biophysique, 91191 Gif-sur-Yvette, Cedex, France.
** Present address: Department of Chemistry, Amherst College, Amherst, MA 01002.

Abbreviations: LDAO, lauryldimethylamine oxide; PMSF, phenylmethylsulfonic acid.

0005-2728/82/0000–0000/$02.75

triplet state of P (^{3}P) and a triplet charge-transfer state (^{3}[P$^+$B$^-$]) [8].

P^F is probably born in a singlet state, as shown in the following scheme:

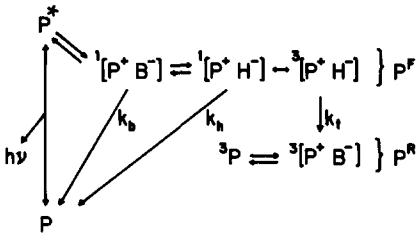

Scheme I.

Regeneration of P* by a back-reaction from state P^F could account for the increase in fluorescence when electron transfer is blocked between H$^-$ and Q. ^{3}P can be formed if the relationship between the unpaired electron spins on the two radicals changes before a back-reaction takes place. Such a change of spin evidently can occur in [P$^+$H$^-$], where the exchange interaction between P$^+$ and H$^-$ is relatively weak [8]. The interaction determines the separation in energy between the singlet and triplet forms of the radical pair, ^{1}[P$^+$ H$^-$] and ^{3}[P$^+$H$^-$]. If the energy gap is small, perturbations such as hyperfine interactions can cause the system to develop triplet character.

Part of the support for Scheme I comes from the observations that weak magnetic fields cause a decrease in the quantum yield of P^R [24–27], and an additional increase in the fluorescence [28,29]. When no field is present, all of the triplet sublevels of [P$^+$H$^-$] evidently are nearly isoenergetic with the singlet state, so that small perturbations can populate any of the sublevels [30,31]. A magnetic field separates two of the triplet sublevels in energy, so that only one sublevel can mix with the singlet state [23–27,32–35]. Werner et al. [34] and Haberkorn and Michel-Beyerle [35] have calculated that hyperfine interactions in [P$^+$H$^-$] could cause sufficiently rapid singlet-triplet mixing to account for the yield of P^R at room temperature. However, there is no experimental evidence that the mixing actually is due to hyperfine interactions, and there has been no convincing explanation of the observation [10,22] that the quantum yield of P^R increases at cryogenic temperatures.

If the additional fluorescence that one sees after reducing Q results from a back reaction from P^F, part of the fluorescence should have approximately the same decay kinetics as P^F. The delayed fluorescence should decrease at low temperatures, if the regeneration of P* from P^F is uphill energetically. It is not clear whether either of these expectations is fulfilled. Shuvalov and Klimov [6] found that the fluorescence from a *Chromatium vinosum* reaction center preparation contained a component with a lifetime of about 6 ns, which decreased in amplitude with decreasing temperature. They attributed the component to a back-reaction and calculated the energy gap between P* and P^F to be 0.12 eV. Van Grondelle et al. [16], who studied the fluorescence of chromatophores and whole cells of several species of bacteria, calculated a similar energy gap. Rademaker and Hoff [36] reevaluated these measurements and concluded that the energy gap is about 0.05 eV. Clayton [15], however, reported that the total fluorescence from purified reaction centers of *Rhodopseudomonas sphaeroides* increased with decreasing temperature down to 200 K, and then became essentially independent of temperature. He concluded that the variable fluorescence probably does not result from a back reaction. Godik and Borisov [17,18] found that the variable fluorescence from chromatophores contains a component with a lifetime of about 5 ns. The fluorescence lifetimes reported by Shuvalov and Klimov [6] and by Godik and Borisov [17,18] are shorter than the lifetime of about 12 ns that has been obtained for P^F in isolated reaction centers [10,20]. Recently, Van Bochove et al. [19] found that the variable fluorescence of chromatophores includes two components, with lifetimes of 5 and 12 ns and with equal initial amplitudes.

In the present work, we measured the decay kinetics of P^F, the quantum yields of P^R, and the lifetimes and yields of fluorescence from isolated reaction centers, under a variety of conditions. We also modified the reaction centers in ways that we expected would alter the rate of singlet-triplet mixing. Scheme I does not account adequately for the results. Preliminary reports of part of this work have been presented [37,38].

Materials and Methods

Fully deuterated cells of wild-type *Rhodospirillum rubrum* were the generous gift of Dr. Henry

Crespi of Argonne National Laboratory. Partially deuterated *Rps. sphaeroides* strain R-26 cells were grown by gradually adapting cultures to a medium made up in 99% ^2H_2O. The medium contained the following (in g/l): succinic acid (4), K_2HPO_4 (2), NaOH (2.5), $(NH_4)_2SO_4$ (1.5), $MgSO_4 \cdot 7H_2O$ (0.2), $CaCl_2 \cdot H_2O$ (0.05), $FeSO_4 \cdot 7H_2O$ (0.01), nicotinic acid (2 mg/l), thiamine hydrochloride (2 mg/l) and biotin (20 μg/l). Harvested cells were stored at −70°C.

Reaction centers of ^1H and ^2H *Rps. sphaeroides* R-26 were prepared as described previously [39], or by the following modification of the procedures described by Clayton and Wang [20] and Wraight [41]. Approx. 150 g packed cells in 100 ml 20 mM Tris-HCl (pH 7.5), 0.1 M NaCl, 5 mM $MgCl_2$, 1 mM PMSF and 1–2 mg DNAase were broken in a French press. Chromatophores were isolated by differential centrifugation, resuspended in a minimal amount of 20 mM Tris-HCl (pH 7.5)/0.1 M NaCl/1 mM PMSF, and stirred overnight at 4°C. The absorbance at 870 nm (A_{870}) was adjusted to 50 with the same buffer. Lauryldimethylamine oxide (LDAO) was added dropwise from a 30% solution with stirring in dim light at 21°C to give a concentration of 0.45% (v/v). The mixture was centrifuged at 300000 × *g* for 2 h (4°C). The supernatant contained no reaction centers. The pellet was resuspended in the same volume of 20 mM Tris-HCl (pH 7.5)/0.1 M NaCl/1 mM PMSF. LDAO was added as before, but to a final concentration of 0.3%, and the preparation was recentrifuged. The reaction centers appeared in the supernatant (A_{800} × volume (ml) ≈ 500), which was decanted and dialyzed at 4°C against 10 mM Tris-HCl (pH 8)/0.1% LDAO/10 μM EDTA/1 mM PMSF. The crude reaction centers were loaded onto a DEAE-Sephacel (Pharmacia) column (1 l bed volume). The column was washed with 2.5 l of the same buffer containing 0.15 M NaCl (21°C) and the reaction centers were eluted with a linear gradient of 0.15–0.35 M NaCl in 4 l of the same buffer. When the blue band containing the reaction centers began to move off the column (0.2–0.25 M NaCl), the salt gradient was stopped and the elution was finished with constant salt concentration. The reaction centers were concentrated on an Amicon ultrafiltration cell with a PM-30 membrane filter and were dialyzed against 10 mM Tris (pH 8)/0.1% LDAO/10 μM EDTA. The A_{280}/A_{800} ratio was typically 1.25–1.35. The detergent then was changed from LDAO to Triton X-100 by dialysis.

Iron-depleted reaction centers were prepared as described previously [39,42]. The iron content, measured by atomic absorption, was 0.28 Fe/reaction center. Quinone-depleted reaction centers were prepared as described by Okamura et al. [12]. In Fig. 4A 93%, and in Fig. 5C 81% of the reaction centers were depleted of Q, as judged from their loss of photochemical activity measured on the millisecond time scale.

Reaction centers of ^1H and ^2H *R. rubrum* were made by a modification of the procedure of Snozzi and Bachofen [43]. Chromatophores were mixed with 1.0% LDAO in 10 mM potassium phosphate (pH 7.0) to give a final LDAO concentration of 0.325% and $A_{880} = 50$, and were centrifuged 1 h at 300000 × *g*. The pellet was resuspended in 0.325% LDAO/10 mM phosphate (pH 7.0) and recentrifuged. The second supernatant was dialyzed (4°C) against 0.02% Triton X-100/10 mM Tris-HCl (pH 8.0), and applied to a DEAE-Sephacel column (4°C), which had been equilibrated with 10 mM Tris-HCl (pH 8.0)/0.05% Triton X-100. The column was washed with one volume of the latter buffer, then with one volume of the same plus 5 mM $Na_2S_2O_4$, followed by a 0–0.5 M NaCl gradient in the same buffer. Fractions containing reaction centers were dialyzed, rechromatographed and stored at −70°C. The deuterated reaction centers still contained a small amount of cytochrome *c*, which did not appear to affect the experiments.

Low redox potentials were achieved by the addition of $Na_2S_2O_4$ (1–2 mg/ml) and high redox potentials by adding $K_3Fe(CN)_6$. To reduce Q^- to Q^{2-}, reaction center suspensions containing $Na_2S_2O_4$ and 0.1 mM horse cytochrome *c* were illuminated for 1 min in a stirred, water-jacketed (10°C) cuvette and then kept in the dark for 10 min [8]. The quinone remained in the doubly reduced state for at least 1 h, as indicated by the comparatively slow decay kinetics of P^R after a flash [8].

Time-resolved fluorescence measurements were made with an RCA 7102 photomultiplier operated at 195 K, protected by a Corning 7-54 glass filter

and a 920 nm interference filter (bandpass 10.5 nm). The signal was captured by a Tektronix R7912 transient digitizer. The computer that controlled the R7912 was used for signal averaging and data analysis. The excitation flashes (834 nm, 3 ns wide) were obtained from a dye laser [10], and were several orders of magnitude below saturation for the photooxidation of P. Signals were averaged over five to ten flashes, spaced 1 min apart. Corrections were made for fluctuations in the flash strength, which was monitored with a photodiode. The photodiode also triggered the R7912.

Measurements of total fluorescence were made with the same photomultiplier and transient digitizer, or with a Biomation 802 digitizer and a home-built signal averager. A high-gain preamplifier was used at the photomultiplier output. The excitation was very weak, 5-μs flashes at 0.2 Hz from a xenon lamp with interference and glass filters giving a bandpass of 30 nm at 595 nm.

A Janis Model 8DT liquid helium dewar (Janis Assoc., Stoneham, MA) was used to control the temperature of the sample. The cuvette was a 2 mm thick chamber between quartz and sapphire windows in a copper block, held at 45°C to the actinic and measuring axes. Temperatures were measured with a gold-0.7 at.% iron vs. chromel thermocouple.

A home-built electromagnet was used for the measurements requiring magnetic fields, and was calibrated with a rotating coil gaussmeter (Rawson Inst., Cambridge, MA). In some experiments, the field was modulated at 1 Hz, and the Biomation digitizer was used for signal averaging of the fluorescence changes in phase with the modulation. Chopped (30 Hz) continuous light (600 nm, 30 $mW \cdot cm^{-2}$) was used for excitation in this case. The photomultiplier was sufficiently far from the magnet, and well shielded, so that the magnetic field did not significantly perturb the response of the tube.

Absorbance changes in response to short pulses of light were measured essentially as described previously [10,21], using the same dewar and cuvette described above. Data for Figs. 3B, 3D and 4 were acquired with single flashes by photographic recording of oscilloscope traces; the remaining data were acquired by averaging 3–10 flashes, using the R7912 transient digitizer.

A non-linear least-squares curve-fitting program based on the Marquart [44] and Grinwald [45] algorithms was used to deconvolve the absorbance and fluorescence signals. The deconvolutions generally involved 400–500 data points, and covered a time interval that was long enough so that P^F or the fluorescence had decayed to less than 2% of its initial level. For both types of measurement, the error in the signal at each data point was dominated by instrumental fluctuations that caused uncertainty in the baseline and in the time of the flash, so that the error was independent of the amplitude of the signal. The major uncertainty was a small (no more than 1 ns) variability in the triggering of the R7912, which correlated with the strength of flash. To evaluate this variability, the deconvolution program shifted the zero-time for the flash in units of one instrumental digital word (approximately 0.1 ns for the fluorescence measurements and 0.4 ns for the absorbance), and then minimized the variance of the data by optimizing the other adjustable parameters. The data points in Figs. 2 and 7 indicate the optimum parameters with the zero-time that gave the lowest variance. The error bars indicate the best parameters when the zero-time was shifted by ± 1 word. The uncertainty in optimizing the other parameters with fixed zero-time was quite small, relative to these error bars. The error bars pertain only to the curve-fitting of individual sets of averaged signals, and do not reflect uncertainties in the repeatability of the measurements; the repeatability can be judged from the scatter of the data points in the figures.

Light-induced EPR spectra were measured at 293 K with a Varian E-9 instrument. The peak-to-peak linewidth of the P^+ signal was 9.8 G in normal *Rps. sphaeroides* R-26 reaction centers and 6.4 in the partially deuterated reaction centers.

Results

Decay kinetics of P^F as a function of temperature

Fig. 1 shows measurements of the absorbance changes that occur when reaction centers from *Rps. sphaeroides* strain R-26 are excited with non-saturating flashes lasting 3 ns. For trace A, the reaction centers were at a moderate redox potential, so that electron transfer from H^- to Q could

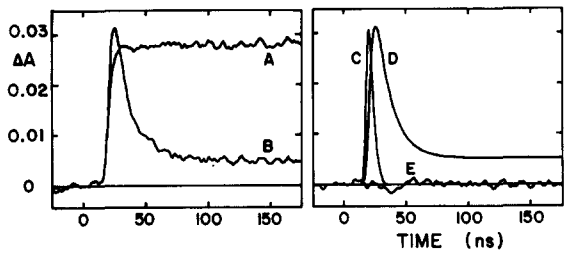

Fig. 1. Absorbance changes caused by flash excitation of 19.5 μM ^{1}H *Rps. sphaeroides* R-26 reaction centers in 50 mM Tris, HCl (pH 8)/0.05% Triton X-100/glycerol (buffer:glycerol, 1:3 w/w), at moderate potential, 277 K (trace A), and low potential, 292 K (trace B). Measuring wavelength = 425 nm, bandpass ≈ 6 nm, excitation wavelength = 834 nm, path ≈ 0.28 cm. Trace C is the excitation function, $E(t)$, obtained from trace A by differentiation and smoothing as described in the text (multiplied by 20 for illustration). Trace D is the calculated signal, $S(t)$, obtained according to Eqn. 1. Trace E is the difference between traces B and D.

proceed normally. The absorbance increase at 425 nm reflects the formation of P^+Q^-. This occurs rapidly [2,3,21] relative to the time scale of the measurements, so the rise of the signal is determined by the width of the flash and the instrumental response time. For trace B, $Na_2S_2O_4$ was added to reduce Q. The absorbance increase in this case reflects the formation of P^F, and the relaxation reflects the decay back to the ground state and to P^R [10]. The asymptote of the decay is a measure of the quantum yield of P^R.

To analyze the decay kinetics of P^F, it was necessary to deconvolve the measured signals from the instrumental response, taking into account the width of the flash. A function describing the instrumental response to the flash, $E(t)$, was obtained by differentiating and smoothing the signal measured at moderate potential (Fig. 1 trace C). (Using the response of the photomultiplier to scattered excitation light for $E(t)$ gave essentially identical results.) Signals like that of trace B then were fit to the convolution function,

$$S(t) = \int_{t'=0}^{t} E(t') \{A \exp[-k(t-t')] + B\} \, dt' \qquad (1)$$

This expression assumes that P^F decays exponentially with an overall rate constant, k. $S(t)$ is the calculated absorbance change (Fig. 1 trace D). A and B are dimensionless adjustable parameters; the initial absorbance change due to the formation of P^F is proportional to $A + B$, and the final absorbance change due to the formation of P^R is proportional to B. The fitting procedure adjusted A, B and k, and also optimized the zero time for $E(t)$ with respect to that of the signal, as described in Materials and Methods.

Measurements similar to those of Fig. 1 were made at temperatures from 4.5 to 300 K. The empty circles in Fig. 2C show the values of k obtained with ordinary (^{1}H) reaction centers in the absence of a magnetic field. The decay rate constant is about $8 \cdot 10^7$ s^{-1} at 280 K, and decreases to about $5 \cdot 10^7$ s^{-1} at low temperatures. Fig. 2D presents similar data for partially deuterated (^{2}H) reaction centers, obtained from cells that had been grown in ^2H_2O. With both ^{1}H and ^{2}H reaction centers, a 650 G magnetic field causes a decrease in k (filled circles in Figs. 2C and D). Figs. 2E and F show the ratio of the values of k in the presence and absence of the field, as functions of temperature. The decrease is about 20% at 280 K, and about 40% at 80 K. We also measured k at 293 K in ^{1}H reaction centers that were depleted of Q; k was essentially the same as in untreated reaction centers.

With ^{1}H reaction centers at 80 K, the decrease in k caused by a magnetic field is half-maximal at about 40 G and is maximal by about 100 G (data not shown). Somewhat stronger fields are required with the ^{2}H reaction centers; a half-maximal effect requires about 100 G.

Quantum yield of P^R

The quantum yield of P^R, relative to that of P^F, is given by $\phi = \{B/(A+B)\}\{\Delta\epsilon_f/\Delta\epsilon_r\}$, where $\Delta\epsilon_f$ and $\Delta\epsilon_r$ are the changes in molar extinction coefficient upon forming P^F and P^R. To determine $\Delta\epsilon_f/\Delta\epsilon_r$, we first measured the absorbance changes at 870 nm and 425 nm for the formation of P^+Q^- and P^R with saturating flashes (834 nm, 30 ns) at 293 K. Because such flashes do not convert all of the reaction centers into P^R [10,31], we scaled the measurements at 425 nm on the assumption that complete conversion into P^R would cause the same bleaching at 870 nm as does the formation of P^+Q^-. This indicated that the formation of P^+Q^- causes (1.60 ± 0.05)-times as large an ab-

sorbance increase at 425 nm as does the formation of P^R. We then compared the absorbance changes at 425 nm for the formation of P^+Q^- and P^F, using 3-ns flashes (834 nm) that were less than 50% saturating. The ratio of these absorbance changes was obtained by the deconvolution procedure described above. The absorbance change associated with P^+Q^- was larger than that associated with P^F, by a factor of 1.12 ± 0.10. Thus, $\Delta\epsilon_f/\Delta\epsilon_r = 1.5 \pm 0.1$ at 293 K.

Figs. 2A and B show the temperature-dependence of the quantum yields calculated on the assumption that $\Delta\epsilon_f/\Delta\epsilon_r = 1.5$ at all temperatures. With both ^1H and ^2H reaction centers, the quantum yield increases with decreasing temperature. The calculated yield is about 0.15 for ^1H reaction centers at 270 K in the absence of a magnetic field, and about 0.7 at 4.5 K. This agrees reasonably well with previous work indicating that ϕ approaches 1.0 at very low temperatures [10,22]. Extrapolation of the curves in Fig. 2A gives a value of about 0.10 for ϕ at 293 K. A 650 G magnetic field decreases the yield by about 50% at 270 K, and by about 10% at 4.5 K (filled circles).

A comparison of the P^R yields in ^1H and ^2H reaction centers should provide information on the role of hyperfine coupling in the interconversion of singlet and triplet states in P^F. Complete replacement of ^1H and ^2H in P^+ and H^- would decrease the effective hyperfine coupling constants by a factor of about 2 [35]. However, the R-26 reaction centers were only partially deuterated, because the cells were grown with ^1H succinate in ^2H_2O. The deuteration reduced the linewidth of the P^+ EPR signal by a factor of about 1.5 (Materials and Methods). Comparison of Figs. 2A and B shows that partial deuteration of the reaction centers had little or no effect on the yield of P^R.

A more accurate comparison of the P^R yields in ^1H and ^2H reaction centers is presented in Fig. 3. These measurements were made at 293 K, using excitation flashes that lasted about 30 ns. The time resolution was lower than it was in the experiments of Figs. 1 and 2, but the sensitivity was higher. Figs. 3A and C show the absorbance changes that accompany the formation of P^+Q^- in reaction centers at moderate redox potential, and those associated with the formation of P^R in reaction centers at low potential, as functions of the flash strength. P^R was measured in both the presence and absence of a magnetic field (filled and open circles). The absorbance changes have been scaled vertically to correct for the difference between the extinction coefficients of P^+Q^- and P^R. At low flash intensities, the horizontal displacement between the curve for P^+Q^- and that for P^R provides a measure of the quantum yield of P^R relative to that of P^+Q^- [39]. Comparison of Figs. 3A and C shows that partial deuteration of the reaction centers has no significant effect on the quantum yield of P^R. In the absence of a magnetic field, the quantum yields measured with both ^1H and ^2H reaction centers were approx. 0.05. Magnetic fields decrease the quantum yields by approx. 50% in both cases.

Figs. 3B and D present similar data for ^1H and ^2H reaction centers from *R. rubrum*. In this case, the cells were essentially completely deuterated. Unlike the reaction centers from *Rps. sphaeroides* R-26, those from *R. rubrum* were obtained from a strain of cells that contains carotenoids. In carotenoid-containing reaction centers, P^R decays rapidly by transferring energy to the carotenoid [20,31]. We measured the product of this process, the carotenoid triplet state, on the assumption that its quantum yield would be proportional to that of P^R. Comparison of Figs. 3B and D shows that, as in the *Rps. sphaeroides* reaction centers, deuteration had no significant effect on the triplet yields. Rademaker et al. [46] also have reported recently that deuteration does not alter the yield of carotenoid triplet states in *R. rubrum* chromatophores.

Deuteration did not affect the rate of electron transfer from Q^- to P^+, as measured from the decay kinetics of absorbance changes in either *Rps. sphaeroides* or *R. rubrum* reaction centers at moderate redox potentials. It did slow the decay of P^R at 77 K in *Rps. sphaeroides*. The rate constants were $7.1 \cdot 10^3$ and $3.6 \cdot 10^3$ s^{-1} in ^1H and ^2H R-26 reaction centers. It also slowed the decay of the carotenoid triplet states. In reaction centers from ^1H *R. rubrum*, the carotenoid triplet decayed with a rate constant of $2.3 \cdot 10^5$ s^{-1}; in the ^2H reaction centers, the rate constant was $1.2 \cdot 10^5$ s^{-1}. In disagreement with Rademaker et al. [46], we found that deuteration had essentially the same effect on the decay kinetics of the triplet states of carotenoids

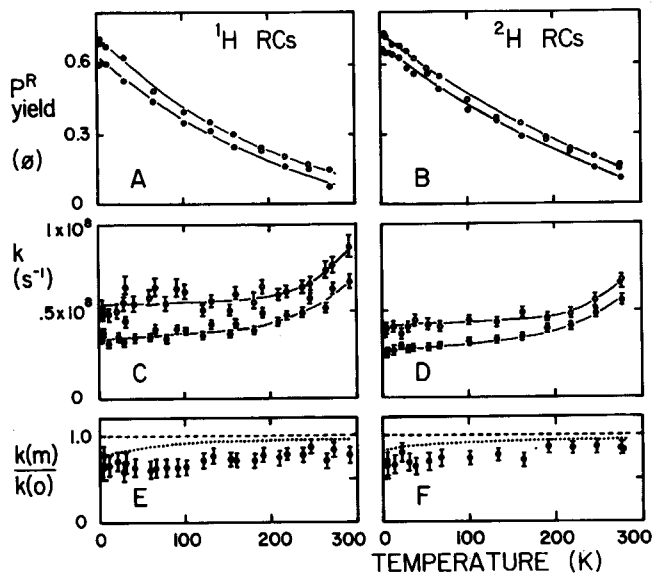

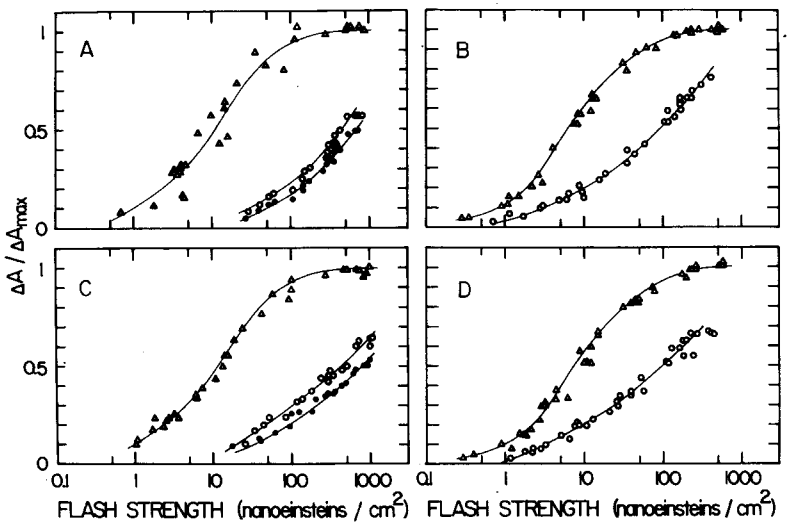

Fig. 2. Relative quantum yield of P^R (ϕ, panels A and B) and rate constant (k, panels C and D) for decay of P^F, as functions of temperature and magnetic field. Obtained by deconvolution of absorbance changes similar to those in Fig. 1B. Open circles, no external magnetic field; closed circles, 650 G field. Panels A, C and E are for ^{1}H R-26 reaction centers (19.5 μM); panels B, D and F are for ^{2}H R-26 reaction centers (13.4 μM). Data from two separate experiments are included in panel C. The meaning of the error bars in C and D is described in Materials and Methods. The error bars in A and B were all smaller than the size of the symbols. Panels E and F: ratio of k measured in the presence and absence of the field, $k(m)$ and $k(0)$, calculated from the data of C and D. The dotted curves in E and F are the predicted ratios, calculated by Eqn. 8 with $k_s/k_t = 0$. The values of $\phi(0)$ and $\phi(m)$ were taken from the curves drawn through the data of A and B. The dashed line, $k(m)/k(0) = 1$, is predicted if $k_s/k_t = 1$. The error bars in E and F were obtained for those in C and D by standard error-propagation theory.

Fig. 3. Light-saturation curves for ^{1}H and ^{2}H *Rps. sphaeroides* R-26 (panels A and C, respectively) and ^{1}H and ^{2}H *R. rubrum* reaction centers (panels B and D, respectively) at 293 K. Triangles represent absorbance changes at 425 nm reflecting the photooxidation of P in reaction centers at moderate potential, normalized by the maximum absorbance change caused by the strongest flash. In panels A and C, the circles represent absorbance changes at 425 nm reflecting the formation of P^R in reaction centers at low potential. Open circles, no magnetic field; filled circles, 650 G field. The absorbance changes for P^R are normalized by the same factor as used for P^+, and also multiplied by the ratio of the differential extinction coefficients for forming P^+ and P^R (1.6). In panels B and D, open circles represent absorbance changes at 575 nm, reflecting the formation of carotenoid triplet in reaction centers at low potential, normalized arbitrarily by assuming that the ratio of extinction coefficients for forming P^+ and the carotenoid triplet is 0.5 at 575 nm. Excitation flashes, 30 ns, 834 nm; cuvette pathlength, 1 cm. A and C, 3.5 μM reaction centers in 50 mM Tris-HCl (pH 8)/0.05% Triton X-100; B and D, 2.6 μM reaction centers in the same buffer.

in the antenna system of *R. rubrum* chromatophores. The rate constants were $2.1 \cdot 10^5\ s^{-1}$ and $1.3 \cdot 10^5\ s^{-1}$ for ^1H and ^2H chromatophores, respectively. These measurements were made by exciting chromatophores with supersaturating 834 nm flashes under anaerobic conditions.

Another perturbation that could play a role in the singlet-triplet mixing in $[P^+H^-]$ is exchange or dipolar coupling between the unpaired electrons of H^- and Q^-. The measurements of P^F and P^R described above were done on reaction centers in which electron transfer from H^- to Q was blocked by the reduction of Q to Q^-. Magnetic interactions of H^- with Q^- are complicated, because Q^- itself interacts with a nearby Fe [42]. The EPR spectrum of H^- changes significantly if the Fe is removed from the reaction center, or if Q^- is reduced to the diamagnetic Q^{2-} [47,48]. To explore the possible role of these interactions in the singlet-triplet mixing, we measured the quantum yield of P^R in reaction centers that were depleted of Q or of Fe (Fig. 4). The measurements were similar to those of Fig. 3, except that it was not necessary to lower the redox potential to detect P^R in the reaction centers that lacked Q. Surprisingly, the quantum yield of P^R in the Q-depleted reaction centers proved to be about twice as great as that in reaction centers containing Q (Fig. 4A). Removal of about 72% of the Fe from the reaction centers caused ϕ to increase about 6-fold (Fig. 4B). The yields in the control experiments with undepleted reaction centers were 0.08 and 0.06 in Figs. 4A and B, respectively.

The results presented in Figs. 3 and 4 indicate that singlet-triplet mixing in P^F does not depend exclusively on either hyperfine interactions or interactions with Q^- or Fe. It is possible, however, that several of these interactions can participate in the mixing, so that the triplet yield is relatively insensitive to a change in any single type of interaction. If the mixing can be driven by either hyperfine interactions or interactions with Q^-, the removal of Q^- might make ϕ more sensitive to deuteration. To test this point, we compared the yields of P^R in ^1H and ^2H reaction centers after reducing Q^- to the diamagnetic Q^{2-} by continuous illumination in the presence of cytochrome *c* (see Materials and Methods). The yields were not significantly different (data not shown).

Total fluorescence as a function of temperature

Figs. 5A and B show the temperature dependence of the fluorescence at 920 nm from ^1H reaction centers at low and moderate redox potentials. At 293 K, reducing Q causes an approximate doubling of the fluorescence. As the temperature is lowered to 77 K, the fluorescence at moderate potential changes very little (closed circles). The fluorescence at low potential first decreases slightly, then increases dramatically, peaks at about 215 K, and finally decreases again (open circles).

A possible explanation for the unusual temperature dependence of the low-potential fluorescence would be that the presence of the negative charge on Q^- affects the primary electron transfer rate in a temperature-dependent manner, perhaps because the distance between P and Q^- varies with temperature. To test this possibility, we examined reaction centers that were depleted of quinones. Fig. 5C shows the temperature dependence of the fluorescence in Q-depleted reaction centers at moderate potential. The curve is similar to that obtained with undepleted reaction centers at low potentials (open circles in Fig. 5B). This indicates that Q^- per se is not responsible for the temperature dependence of the fluorescence; the essential requirement evidently is only that electron transfer from H^- to Q be blocked. The change in the fluorescence with temperature is a somewhat smaller fraction of the total fluorescence in Fig. 5C than it is Fig. 5B; this could be due to the fact that about 20% of the reaction centers still contained Q (Materials and Methods). These reaction centers would contribute a temperature-independent fluorescence at moderate potential (cf. filled circles in Fig. 5B).

Fig. 5D shows measurements similar to those of Fig. 5B except that 1 mM *o*-phenanthroline was present. The fluorescence at low temperatures was more intense at both low and moderate potential. This suggests that *o*-phenanthroline slows the primary electron transfer reaction, especially at low temperatures.

In the experiments of Fig. 5, the detection wavelength was fixed at 920 nm; no correction was made for the shifting and sharpening of the emission spectrum that occurs with decreasing temperature [15]. This correction would be small, because the ratio of the areas under the emission spectra at

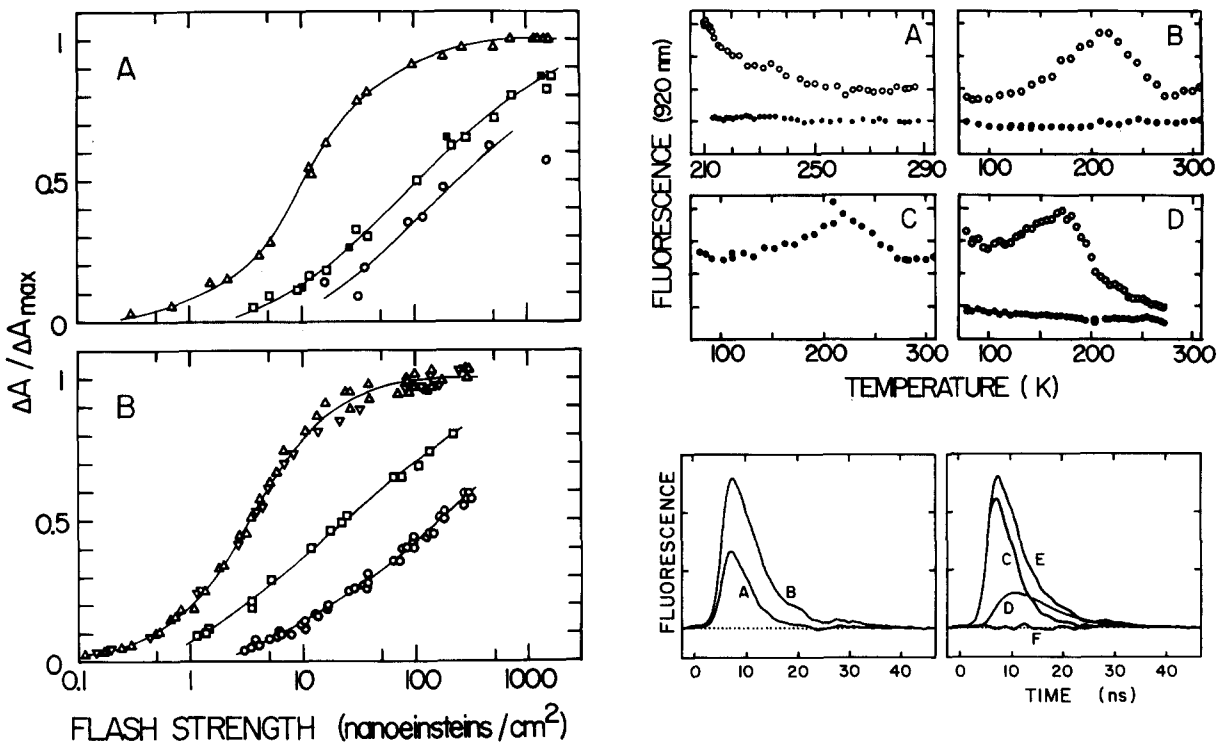

Fig. 4. Light-saturation curves for partially Q-depleted (panel A) and Fe-depleted (panel B) *Rps. sphaeroides* R-26 reaction centers. Absorbance changes were measured at 425 nm and normalized as in Figs. 3A and C. In panel A, triangles represent absorbance changes reflecting the photooxidation of P, measured at moderate potential in reaction centers that were not depleted of Q; open and filled squares, P^R formation in Q-depleted reaction centers at moderate and low-potentials, respectively; circles, P^R formation at low-potential in reaction centers not depleted of Q. In panel B, triangles are for P^+ formation at moderate potential in Fe-depleted (△) and undepleted (▽) reaction centers; squares, P^R formation in Fe-depleted reaction centers at low potential; circles, P^R formation at low potential in reaction centers not depleted of Fe. Excitation flashes were 30 ns, 694 nm (panel A) and 834 nm (panel B); cuvette pathlength, 1 cm. Panel A, 2.5 μM reaction centers; panel B, 7.2 μM Fe-depleted and 6.3 μM undepleted reaction centers; buffer as in Fig. 3.

Fig. 5. Total fluorescence at 920 nm from ^{1}H R-26 reaction centers vs. temperature. ○, low potential; ●, moderate potential. Panel A: 12.0 μM reaction centers in 50 mM Tris-HCl (pH 8)/0.05% Triton X-100/glycerol (buffer:glycerol, 1:2.5, w/w). Panel B: 8.0 μM reaction centers in 10 mM Tris-HCl (pH 8)/0.05% Triton X-100. Freezing of the solution caused the apparent fluorescence to increase by about 20% near 273 K; the data are normalized to remove this discontinuity. Panel C: 8.0 μM Q-depleted reaction centers at moderate potential in 10 mM Tris-HCl (pH 8)/0.05% Triton X-100. Panel D: same as B but with 1 mM *o*-phenanthroline. The amounts of fluorescence in the four panels cannot be compared directly, since the apparatus was disassembled between experiments. Cuvette path: 1 cm for panel A; 0.28 cm for the others.

Fig. 6. Time-resolved fluorescence at 920 nm from ^{1}H R-26 reaction centers. (5.9 μM reaction centers in 10 mM Tris-HCl (pH 8)/0.05% Triton X-100 at 292 K) at moderate redox potential (trace A) and low potential (B). Trace E shows the calculated signal, $F_L(t)$, obtained by deconvolution of B according to Eqn. 2. For the deconvolution, trace A was used as $F_M(t)$, and k_β was fixed at $1.67 \cdot 10^8$ s^{-1}. Trace C is the calculated prompt fluorescence, $\alpha F_M(t)$, and D the calculated delayed fluorescence, $\int_0^t F_M(t')\{\beta \exp[-k_\beta(t-t')]\}\, dt'$. *F* is the difference between E and B.

77 and 293 K was close to the ratio of the emission intensities at 920 nm (data not shown).

Time-resolved fluorescence measurements

Fig. 6 shows time-resolved measurements of the fluorescence at 292 K from reaction centers at moderate and low redox potentials. In agreement with Fig. 5, the total amount of fluorescence approximately doubles when Q is reduced; the lifetime of the fluorescence also increases noticeably.

At high potentials, when P is oxidized, the fluorescence intensity decreases to about 12% of that at moderate redox potentials (not shown).

To analyze the decay kinetics of the fluorescence at low redox potentials, we fit the signals to convolution functions of the form

$$F_L(t) = \alpha F_M(t) + \int_{t'=0}^{t} F_M(t') \times \{\beta \exp[-k_\beta(t-t')]\}\, dt' \quad (2)$$

Here $F_L(t)$ is the calculated fluorescence signal at low potentials (Fig. 6, trace E); $F_M(t)$, the measured fluorescence signal at moderate potentials (Fig. 6A); α, a dimensionless adjustable parameter; and β, a parameter with units of s^{-1}. Because the fluorescence lifetime at moderate potentials is very short [1,49], $F_M(t)$ is kinetically equivalent to the response of the detection apparatus to the excitation flash. (A scaled measurement of scattered excitation light was, in fact, superimposable on $F_M(t)$.) $\alpha F_M(t)$ represents the instrumental response to the 'prompt' fluorescence at low potentials (Fig. 6C), and $\int_0^t F_M(t') \times \{\beta \exp[-k_\beta(t-t')]\}\, dt'$ represents the response to the 'delayed' fluorescence, which is assumed to decay exponentially with rate constant k_β (Fig. 6D). We also fit the data with deconvolution functions that included a double-exponential decay for the delayed fluoresence, in addition to the term for prompt fluorescence. Because of the larger number of adjustable parameters, the double-exponential fits expectedly had lower variances than the single-exponential fits. However, the improvement was probably not significant, considering the uncertainty due to variation in the zero-time of the flash. (The lifetimes of the two delayed fluorescence components obtained by the double-exponential fits were on the order of 2 and 10 ns. The initial amplitude of the shorter-lived component was generally about 5-times that of the longer.)

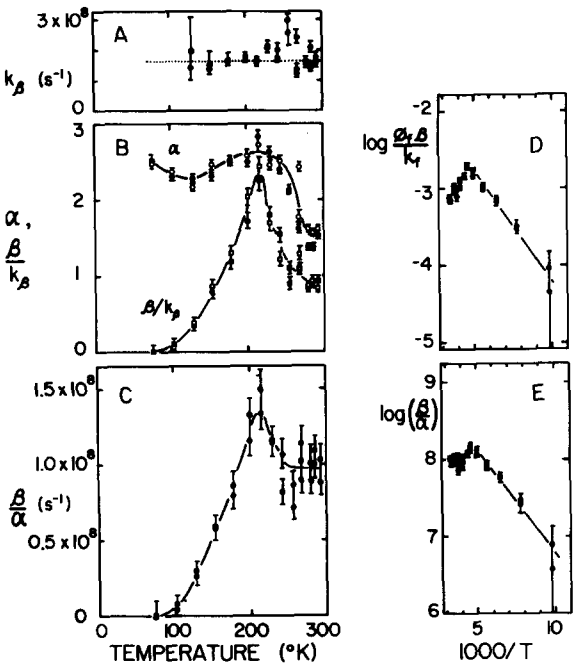

Fig. 7. Parameters obtained by deconvolution on the time-resolved fluorescence measurements, as functions of temperature. Open symbols: no magnetic field. Filled symbols: 650 G field. The meaning of the error bars is described in Materials and Methods. A, delayed fluorescence decay rate constant, k_β. For the deconvolutions summarized in panels B–E, k_β was fixed at $1.67 \cdot 10^8\ s^{-1}$ (dotted line in panel A). B, integrated amplitude of the prompt fluorescence (α, circles), and of the delayed fluorescence (β/k_β, squares) C and E, ratio β/α (interpreted as k_{-1} in the text). D, $\phi_f\beta/k_f$ (interpreted as K_{eq} in the text) calculated with $\phi_f = 4 \cdot 10^{-4}$ and $k_f = 8 \cdot 10^7\ s^{-1}$.

Fig. 7A shows the values of k_β, the decay rate constant obtained by single-exponential fits of the fluorescence, over the tempeature range 128–292 K. At lower temperatures, the amplitude of the delayed fluorescence was too low to allow a reliable determination of k_β. The empty circles are measurements made in the absence of a magnetic field; the filled circles, measurements in the presence of a 650 G field. Although the data are scattered, k_β is about twice as large as the rate constant (k) obtained for the decay of P^F (Fig. 2). The lifetime of the delayed fluorescence ($1/k_\beta$) is approx. 6 ns, in agreement with the lifetimes that Shuvalov and Klimov [6], Godik and Borisov [17,18], and Van Bochove et al. [19] have measured in chromatophores and in *C. vinosum* reaction centers. k_β appears not to depend greatly on temperature, or on magnetic fields. However, the uncertainty in the measurements would obscure changes in k_β that were less than approx. 50%.

The contributions that the prompt fluorescence (P.F.) and delayed fluorescence (D.F.) make to the total fluorescence yield are obtained by integrating

from $t = 0$ to ∞:

$$(\text{P.F.}) = \int_{t=0}^{\infty} F_M(t)\,dt = \alpha \int_0^{\infty} F_M(t)\,dt \tag{3a}$$

$$(\text{D.F.}) = \int_{t=0}^{\infty}\int_{t'=0}^{t} F_M(t')\,\beta \exp[-k_\beta(t-t')]\,dt'\,dt$$

$$= (\beta/k_\beta)\int_0^{\infty} F_M(t)\,dt \tag{3b}$$

The ratio of these integrals is $\alpha : \beta/k_\beta$. The ratios of the integrated prompt and delayed fluorescence at low potentials to the total fluorescence at moderate potentials are α and β/k_β, respectively. Fig. 7B shows the temperature dependence of α and β/k_β. In order to obtain values for α and β over as wide a range of temperatures as possible, the deconvolutions for this figure were done with k_β held fixed at $1.67 \cdot 10^8\ s^{-1}$ ($1/k_\beta = 6$ ns). This reduced the number of adjustable parameters in the deconvolution program from 4 to 3 (α, β and the zero-time), at the expense of relatively small increases in the variance of the fits at the temperatures above 130 K where the full, four-parameter program was reliable.

At 293 K, the prompt part of the low-potential fluorescence (α) is about 1.5-times the moderate-potential fluorescence. As the temperature is lowered to 200 K, α increases by about 70% (Fig. 7B). The increase contrasts with the behavior of the moderate-potential fluorescence, which remains constant over this temperature range (Fig. 5A and B). Below 200 K, α becomes relatively insensitive to temperature (Fig. 7B). The integrated delayed fluorescence at 293 K is comparable to the total fluorescence at moderate potentials ($\beta/k_\beta \approx 1.0$). β/k_β increases with decreasing temperature down to about 200 K, but then falls essentially to zero by 75 K (Fig. 7B).

In Fig. 7 there is no obvious effect of a magnetic field on either of the fluorescence components. We therefore looked for changes in total fluorescence by a more sensitive technique that used a modulated magnetic field. With reaction centers at low potential at 293 K, a 650 G field caused an increase of approx. 1.6% in the total fluorescence at 920 nm. This is smaller than the 5–6% increase observed by Voznyak et al. [29], and is too small to be detectable in our time-resolved measurements. There was no detectable effect (less than 0.05%) on the fluoresence at moderate potential.

Discussion

*The rate of back-reactions from P^F to P**

The delayed fluorescence from isolated reaction centers at low redox potentials is probably due to a back-reaction that regenerates P* from P^F. But the delayed fluorescence decays about twice as rapidly as does P^F. A relaxation with a time constant of approx. 6 ns evidently occurs after the formation of P^F. The relaxation must either decrease the probability of the back reaction, or decrease the probability that P*, once regenerated, will fluoresce. We have no basis for deciding between these two alternatives, although the former seems more likely.

One can estimate an effective rate constant for the back-reaction that regenerates P*, by using the following simplified kinetic scheme:

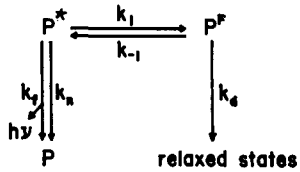

Scheme II.

In Scheme II, P* decays to P by fluorescence (k_f) and by nonradiative paths (k_n), with a lumped rate constant $k_0 = k_f + k_n$. P* is converted to P^F with rate constant k_1, and regenerated with k_{-1}. P^F decays to P and P^R, or relaxes in other ways that inhibit its return to P*, with a lumped rate constant k_d. Suppose initially that the 6 ns decay of the delayed fluorescence is due primarly to a relaxation that prevents the return of P^F to P*. k_f and k_n are taken to be the same when P* is regenerated from P^F as they are when P* is initially formed, and are assumed not to change as P^F relaxes.

The use of first-order rate constants to describe the reactions of P^F also assumes that P^F is kinetically homogeneous. This cannot be strictly correct, because the fraction of P^F that is in a singlet state changes with time. Only the singlet radical pairs can return to P* or P, and only the triplet radical

pairs can proceed to P^R. We found, however, that the observed decay kinetics of P^F and of the delayed fluorescence can be described satisfactorily by single first-order rate constants at all temperatures (Figs. 1, 2, 6 and 7). In addition, the conversion of $^3[P^+H^-]$ to P^R probably is fast, compared to the conversion of $^1[P^+H^-]$ to $^3[P^+H^-]$. The principal evidence for this is the observation by Chidsey et al. [27] that the P^R yield increases in the presence of extremely strong magnetic fields. Unlike the weak fields that we used, very strong fields are expected to increase the rate of the singlet-triplet mixing in P^F. This would increase ϕ only if the mixing is rate-limiting. P^F therefore always consists mainly of singlet radical pairs, and will behave nearly homogeneously as far as the back-reaction to P* is concerned. As discussed below, the effects of weak magnetic fields on the decay kinetics of P^F and the quantum yield of P^R also support the view that the conversion of $^3[P^+H^-]$ to P^R is fast compared to the paths by which P^F decays to the singlet ground state. Kinetic models that incorporate the time-dependence of singlet-triplet mixing in P^F have been developed by Haberkorn et al. [35] and Rademaker and Hoff [36]. The use of such a model would require the introduction of additional parameters that have not been measured directly. This seems unwarranted for the present discussion, in view of the limited time-resolution of our measurements, and the uncertainties that remain concerning the mechanisms of the singlet-triplet mixing and the quenching of the delayed fluorescence.

In Scheme II, the decay of P* after a δ-function flash will be described by two exponentials:

$$P^*(t)=[P_0^*]\left\{\frac{(k_1+k_0-L_2)}{(L_1-L_2)}\exp(-L_1t)+\frac{(L_1-k_1-k_0)}{(L_1-L_2)}\exp(-L_2t)\right\} \quad (4)$$

where $[P_0^*]$ is the initial concentration of P*, $L_1 = (X+Y)/2$, $L_2=(X-Y)/2$, $X=k_1+k_{-1}+k_0+k_d$, and $Y=[X^2-4(k_1k_d+k_0k_{-1}+k_0k_d)]^{1/2}$. The rate of fluorescence at any time is $k_fP^*(t)$. The first exponential in Eqn. 4 thus gives 'prompt' fluorescence (P.F.) with a lifetime of $1/L_1$; the second gives 'delayed' fluorescence (D.F.) with a lifetime of $1/L_2$. The contribution of each term to the total fluorescence is obtained by integrating from $t=0$ to ∞, and the ratio of the delayed and prompt fluorescence is the ratio of these integrals:

$$(\text{D.F.})/(\text{P.F.})=\frac{(L_1-k_1-k_0)\,(L_1)}{(k_1+k_0-L_2)\,(L_2)} \quad (5)$$

From the measurements of the decay kinetics of P^F and delayed fluorescence described above, from recent picosecond absorbance measurements [4,5], and from the high quantum yield of photochemistry [50] it is clear that $k_1 \gg k_0, k_d$. Provided that k_{-1} is not too large with respect to k_d, Eqn. 5 then simplifies to:

$$(\text{D.F.})/(\text{P.F.})\approx k_{-1}/L_2,$$

$$\text{or } k_{-1}=L_2\,(\text{D.F.})/(\text{P.F.}) \quad (6)$$

The parameters on the right side of Eqn. 6 can be obtained from the deconvolutions of the fluorescence data. The deconvolution takes into account the actual width of the excitation flashes, as well as the response time of the detection apparatus. Equating L_2 with k_β and (D.F.)/(P.F.) with $\beta/k_\beta\alpha$ (Eqn. 3) gives $k_{-1}=\beta/\alpha$. Figs. 7C and E show plots of β/α as a function of temperature: 7C is a linear plot and 7E an Arrhenius plot. The calculated rate constant is about $10^8\ s^{-1}$ at room temperature. It increases slightly with decreasing temperature down to 215 K, and then falls. The apparent activation energy in the low-temperature region is 0.03 ± 0.01 eV.

The maximum value of k_{-1} is obtained at about 215 K, and is on the order of $1.5 \cdot 10^8\ s^{-1}$. This is about 2-times larger than the measured decay rate constant for P^F (Fig. 2C), and is about the same as the rate constant (k_β) for the decay of the delayed fluorescence. P* thus appears to be regenerated only once or twice during the lifetime of P^F. If $k_0 \approx 5 \cdot 10^8\ s^{-1}$ and $k_1 \approx 3 \cdot 10^{11}\ s^{-1}$, the probability that P* will decay to the ground state is approx. $1.7 \cdot 10^{-3}$. More usually, P* simply returns to P^F. This means that only about 0.3% of the decay of P^F occurs via P* at 215 K, and even less at other temperatures.

The conclusion that little of the decay of P^F occurs via P* would not be affected materially if

one interpreted the quenching of the delayed fluorescence in terms of a change in the probability that P* fluoresces, rather than in the probability that P* is regenerated from P^F. On this model, L2 could be equated with k, the rate constant for the decay of P^F. Eqn. 6 would apply to the integrated delayed fluorescence that one would expect to obtain in the absence of the change in the fluorescence yield from P*, which would be β/k. Thus $k_{-1} = \beta/\alpha$ in this model also.

Standard free energy and enthalpy gaps between P and P^F*

If there are intermediate states between P* and P^F, the 'prompt' fluorescence itself will be multiexponential. The apparent rate constant k_{-1} can still be used to characterize the back reaction, but both k_1 and k_{-1} will be made up of several microscopic rate constants. We know, however, that an initial equilibrium between P* and P^F is reached in about 4 ps [4], which is very short compared to the lifetime of P^F. In this situation, the intensity of the delayed fluorescence from P^F will be proportional to k_f, to $[P^F]$, and to an equilibrium constant $K_{eq} = [P^*]/[P^F]$. (This assumes again that P^F is kinetically homogeneous.) Because the total yield of fluorescence is very small compared to that from free bacteriochlorophyll [1], K_{eq} must be quite small. If the form of P^F that is responsible for the delayed fluorescence is created with a quantum yield close to 1.0, and decays with the effective rate constant k_β, the integrated amount of delayed fluorescence after a δ-function flash will be approx. $k_f K_{eq}[P_0^*]/k_\beta$. The ratio of the integrated delayed fluorescence to the total fluorescence at moderate potentials will be $k_f K_{eq}[P_0^*]/k_\beta \phi_f [P_0^*] = k_f K_{eq}/\phi_f k_\beta$, where ϕ_f is the quantum yield of the fluorescence at moderate potentials. Setting this ratio equal to β/k_β (Eqn. 3) gives

$$K_{eq} = \phi_f \beta / k_f \qquad (7)$$

Again, the deconvolution takes into account the width of the flash. Eqn. 7 has been used to analyze the delayed fluorescence from reaction centers in the state P^+Q^- [51].

Zankel et al. [1] have measured ϕ_f to be $(4.0 \pm 1.5) \cdot 10^{-4}$ at 293 K. k_f can be calculated by the Strickler-Berg [52] relationship. Using $1.3 \cdot 10^5$ $M^{-1} \cdot cm^{-1}$ for the extinction coefficient of P at 865 nm [53] and 1.5 for the refractive index, and assuming that P* and P have similar partition coefficients, defined with respect to the lowest vibrational levels of the two states [51], one obtains $k_f \simeq 8 \cdot 10^7$ s^{-1}. k_f decreases slightly, but negligibly, with decreasing temperature.

Fig. 7D shows a van't Hoff plot of K_{eq} calculated by Eqn. 7. At 290 K, K_{eq} is about 10^{-3}. Like k_{-1}, K_{eq} increases slightly with decreasing temperature down to about 215 K, and then falls. From K_{eq}, the standard partial molecular free energy difference between P* and P^F is calculated to be about 0.11 eV at 215 K, and 0.25 eV at 290 K. From the slope of the van't Hoff plot, the standard enthalpy of P^F appears to be 0.03 ± 0.01 eV above that of P* at room temperature, and 0.03 ± 0.01 eV below it at low temperatures. These estimates of the free energy and enthalpy differences apply to the state of P^F preceding the relaxation that quenches the delayed fluorescence, and they do not depend on the nature of the relaxation. The enthalpy gaps of about 0.03 eV calculated from the decrease of k_{-1} and K_{eq} at low temperatures are similar to the 0.025 eV gap that has been calculated between the $^1[P^+B^-]$ and $^1[P^+H^-]$ forms of P^F [8]. The free energy gap between P* and P^F at room temperature has been estimated previously from the apparent midpoint redox potentials of P and I in chromatophores of *Rps. viridis*; the estimates range from 0.1 to 0.3 eV [47,54–56].

The nonlinear van't Hoff plot of K_{eq} could mean that the formation of P^F from P* involves a change in the heat capacity of the reaction center, perhaps due to a change in molecular or intermolecular vibrational frequencies. Another possible interpretation of the unusual temperature dependence is that, at high temperatures, P^F undergoes a very rapid relaxation that decreases the probability of the back-reaction that regenerates P*. We would not observe such a relaxation directly if it occurred in much less than 1 ns. If the relaxation diminished in extent with decreasing temperature, the delayed fluorescence could increase. It is possible that the temperature dependence of K_{eq} reflects a phase transition of bound water. The kinetics of the back-reaction from P^+

Q^- to PQ increase in rate with decreasing temperature in ordinary reaction centers, but not in photochemically active reaction centers that have been dehydrated [57].

Although an increase in fluorescence with decreasing temperatures has not been observed in chromatophores or whole cells, measurements reported by van Grondelle et al. [16] do show an inflection point near 200 K. Also, the effect of magnetic fields on the delayed fluorescence of chromatophores and reaction centers increases with decreasing temperature down to 250 K [28,29].

A possible interpretation of the 6 ns relaxation is that it reflects an equilibration between the singlet radical pair, $^1[P^+H^-]$, and the three substates of $^3[P^+H^-]$. Such an equilibration could account for about a 4-fold decrease in K_{eq}. But this interpretation would be inconsistent with the evidence that the singlet-triplet mixing is rate-limiting for the formation of P^R. In addition, if the decay of the delayed fluorescence reflected singlet-triplet equilibration, external magnetic fields should decrease k_β by about a factor of 3, and should double the amplitude of the delayed fluorescence that remains after the relaxation. Within our experimental error, magnetic fields had no effect on k_β or on the extent of the decay. An alternative interpretation of the 6 ns relaxation is that it reflects nuclear movements in P^F, following the initial charge separation.

The quantum yield of P^R

From the discussion above, most of the decay of P^F must occur by paths that do not require the regeneration of P*. One of these paths generates the triplet state P^R. We considered two possible mechanisms of the spin rephasing that leads to P^R: hyperfine interactions and magnetic interactions involving Q^- or Fe. The quantum field of P^R was not decreased by the extraction of Q^- or Fe from the reaction centers, or by deuteration when the reaction centers contained either Q^- or Q^{2-}. In fact, removing either Q^- or Fe caused ϕ to increase. These observations leave the origin of the singlet-triplet mixing unclear. The increase in ϕ resulting from the extraction of Q could be explained on the suggestion [8] that a negative charge on Q increases the energy of $^1[P^+H^-]$ with respect to $^1[P^+B^-]$. If the exchange interaction between P^+ and B^- is much greater than that between P^+ and H^-, singlet-triplet mixing will occur at a significant rate only in P^+H^- [8].

Weak magnetic fields decrease both ϕ and the overall rate constant k for the decay of P^F (Fig. 2). This is qualitatively consistent with Scheme I, no matter what the mechanism and rate of singlet-triplet mixing, provided that k_t is greater than k_b and k_h. Quantitatively, however, the effect of magnetic fields on k is larger than one would expect it to be. At 290 K, the formation of P^R accounts for only 5–10% of the decay of P^F in the absence of a magnetic field, and about half as much in the presence of a field. One would therefore expect the field to slow the decay of P^F by only about 2.5–5%. The observed decrease in k is about 20%.

Figs. 2E and F illustrate this discrepancy in more detail. According to Scheme I, $^1[P^+B^-]$ decays directly to the ground state with rate constant k_b. $^1[P^+H^-]$ can decay directly or by way of $^1[P^+B^-]$; the latter path probably predominates, except at very low temperatures [8]. If $^1[P^+B^-]$ and $^1[P^+H^-]$ are in rapid equilibrium [4,8], with $^1[P^+B^-]/^1[P^+H^-] = K_{bh}$, the effective rate constant for the decay of the two singlet radical pairs is $k_s = (k_b K_{bh} + k_h)/(1 + K_{bh})$. The triplet radical pair $^3[P^+H^-]$ decays to P^R with rate constant k_t. In this situation, the overall decay rate constant k can be related to ϕ, k_s and k_t by the expression [35,36]: $1/k = \phi/k_t + (1-\phi)/k_s$. (This expression is quite general, and does not assume that P^F is kinetically homogeneous.) If the field does not affect k_s or k_t, the ratio of the rate constants measured in the presence and absence of the field, $k(m)$ and $k(0)$, should be

$$\frac{k(m)}{k(0)} = \frac{1-(1-k_s/k_t)\,\phi(0)}{1-(1-k_s/k_t)\,\phi(m)} \qquad (8)$$

where $\phi(m)$ and $\phi(0)$ are the quantum yields of P^R in the presence and absence of the field. The dotted lines in Figs. 2E and F show the predicted $k(m)/k(0)$ ratios. These were calculated from the $\phi(0)$ and $\phi(m)$ values of Figs. 2A and B with $k_s/k_t = 0$, which gives the largest possible predicted effect of the field. The observed effects are too great to be consistent with Eqn. 8, for any possible value of k_s/k_t.

In addition, Scheme I has difficulty accounting

for the increase in ϕ that occurs at low temperatures. The increase cannot be explained simply by assuming that k_s decreases with decreasing temperature, because pronounced changes in ϕ occur at temperatures below 150 K, where k is relatively insensitive to the temperature (Fig. 2). It cannot be explained by a decrease in the amount of P^F that decays by the competing path via P*, because this amount is negligible even at high temperatures. One could assume that the singlet-triplet mixing rate increases with decreasing temperature, but there is no independent evidence for this.

A possible solution to these difficulties is that P^F has a decay pathway that requires singlet-triplet mixing but does not result in the formation of P^R. Such a path could involve the conversion of $^3[P^+H^-]$ to a different triplet state that decays to the ground state so rapidly that it is not detectable. The formation of P^R then would represent only a fraction $(1/r)$ of the decay of $^3[P^+H^-]$. The total triplet yield would be ϕr, where ϕ, as before, is the observed yield of P^R. Values of r near 3 can account for the observed values of $k(m)/k(0)$ near room temperature. The temperature dependence of ϕ and of $k(m)/k(0)$ could be explained if r decreased linearly to about 1.1 with a decrease in temperature to 4 K. One feature of this model is that the corrected triplet yield (ϕr), instead of increasing continually with decreasing temperature as ϕ does (Figs. 2A and B), increases with decreasing temperature down to about 80 K and then plateaus at a value of about 0.8. This temperature dependence could be rationalized simply, along with the observed temperature-dependence of k, by an activation energy of about 0.025 eV for the decay of P^F via $^1[P^+B^-]$. The formation of $^1[P^+B^-]$ from $^1[P^+H^-]$ requires an energy increase of about 0.025 eV [8].

In conclusion, although Scheme I seems satisfactory in outline, it does not account adequately for the decay kinetics and temperature dependence of the delayed fluorescence, nor for the effects of magnetic fields and temperature on the yield of P^R and the decay kinetics of P^F. We have suggested possible explanations for some of the discrepancies.

Acknowledgements

We thank Dr. C. Wraight for advice on reaction center preparations, Drs. H. Crespi and J. Norris for providing deuterated *R. rubrum*, Dr. V. Shuvalov for helpful discussion, and J. Slater and J. Rutberg for preparing reaction centers. The work was supported by NSF grant PCM-77-13290, and by the Science and Education Administration of the U.S. Department of Agriculture under Grant No. 5901-0419-8-0025 from the Competitive Research Grants Office.

References

1 Zankel, K.L., Reed, D.W. and Clayton, R.K. (1968) Proc. Natl. Acad. Sci. USA 61, 1243–1249
2 Rockley, M.G., Windsor, M.W., Cogdell, R.J. and Parson, W.W. (1975) Proc. Natl. Acad. Sci. USA 72, 2251–2255
3 Kaufmann, K.J., Dutton, P.L., Netzel, T.L., Leigh, J.S. and Rentzepis, P.M. (1975) Science 188, 1301–1304
4 Holten, D., Hoganson, C., Windsor, M.W., Schenck, C.C., Parson, W.W., Migus, A., Fork, R.L. and Shank, C.V. (1980) Biochim. Biophys. Acta 592, 461–477
5 Shuvalov, V.A., Klevanik, A.V., Sharkov, A.V., Matveetz, Yu.A. and Krukov, P.G. (1978) FEBS Lett. 91, 135–139
6 Shuvalov, V.A. and Klimov, V.V. (1976) Biochim. Biophys. Acta 440, 587–599
7 Dutton, P.L., Prince, R.C., Tiede, D.M., Petty, K.M., Kaufmann, K.J., Netzel, T.L. and Rentzepis, P.M. (1977) Brookhaven, Symp. Biol. 28, 213–237
8 Shuvalov, V.A. and Parson, W.W. (1981) Proc. Natl. Acad. Sci. USA 78, 957–961
9 Dutton, P.L., Leigh, J.S. and Seibert, M. (1972) Biochem. Biophys. Res. Commun. 46, 406–413
10 Parson, W.W., Clayton, R.K. and Cogdell, R.J. (1975) Biochim. Biophys. Acta 387, 265–278
11 Cogdell, R.J., Brune, D.C. and Clayton, R.K. (1974) FEBS Lett. 45, 344–347
12 Okamura, M.Y., Isaacson, R.A. and Feher, G. (1975) Proc. Natl. Acad. Sci. USA 72, 3491–3495.
13 Reed, D.W., Zankel, K.L. and Clayton, R.K. (1969) Proc. Natl. Acad. Sci. USA 63, 42–46
14 Slooten, L. (1972) Biochim. Biophys. Acta 256, 452–466
15 Clayton, R.K. (1977) in Photosynthetic Organelles: Structure and Function (Miyachi, S., Katoh, S., Fujita, Y. and Shibata, K., eds.), special issue of Plant Cell Physiology, No. 3, pp. 87–96
16 Van Grondelle, R., Holmes, N.G., Rademaker, H. and Duysens, L.N.M. (1978) Biochim. Biophys. Acta 503, 10–25
17 Godik, V.I. and Borisov, A.Y. (1979) Biochim. Biophys. Acta 548, 296–308
18 Godik, V.I. and Borisov, A.Y. (1980) Biochim. Biophys. Acta 590, 182–193

19 Van Bochove, A.C., Van Grondelle, R. and Duysens, L.N.M. (1981) Proceedings of 5th International Congress on Photosynthesis (Akoyunoglou, G., ed.), International Science Services, Jerusalem, in the press
20 Cogdell, R.J., Monger, T.G. and Parson, W.W. (1975) Biochim. Biophys. Acta 408, 189–199
21 Holten, D., Windsor, M.W., Parson, W.W. and Thornber, J.P. (1978) Biochim. Biophys. Acta 501, 112–126
22 Wraight, C.A., Leigh, J.S., Dutton, P.L. and Clayton, R.K. (1974) Biochim. Biophys. Acta 333, 401–408
23 Leigh, J.S. and Dutton, P.L. (1974) Biochim. Biophys. Acta 357, 67–77
24 Blankenship, R.E., Schaafsma, T.J. and Parson, W.W. (1977) Biochim. Biophys. Acta 461, 297–305
25 Hoff, A.J., Rademaker, H., van Grondelle, R. and Duysens, L.N.M. (1977) Biochim. Biophys. Acta 460, 547–554
26 Michel-Beyerle, M.E., Scheer, H., Seidlitz, H., Tempus, D. and Haberkorn, R. (1979) FEBS Lett. 100, 9–12
27 Chidsey, C.E.D., Roelofs, M.G. and Boxer, S.G. (1980) Chem. Phys. Lett. 74, 113–118
28 Rademaker, H., Hoff, A.J. and Duysens, L.N.M. (1979) Biochim. Biophys. Acta 546, 248–255
29 Voznyak, V.M., Elfimov, E.I. and Sukovatitzina, V.K. (1980) Biochim. Biophys. Acta 592, 235–239
30 Hoff, A.J. and Gorter de Vries, H. (1978) Biochim. Biophys. Acta 503, 94–106
31 Parson, W.W. and Monger, T.G. (1976) Brookhaven Symp. Biol. 28, 195–211
32 Thurnauer, M.C., Katz, J.J. and Norris, J.R. (1975) Proc. Natl. Acad. Sci. USA 72, 3270–3274
33 Levanon, H. and Norris, J.R. (1978) Chem. Rev. 78, 185–198
34 Werner, H.-J., Schulten, K. and Weller, A. (1978) Biochim. Biophys. Acta 502, 255–268
35 Haberkorn, R. and Michel-Beyerle, M.E. (1979) Biophys. J. 26, 489–498
36 Rademaker, H. and Hoff, A.J. (1981) Biophys. J. 34, 325–344
37 Blankenship, R.E. and Parson, W.W. (1977) Abstracts of the 4th International Congress on Photosynthesis, p. 37, The Biochemical Society, London
38 Blankenship, R.E. and Parson, W.W. (1979) Biophys. J. 25, 205a
39 Blankenship, R.E. and Parson, W.W. (1979) Biochim. Biophys. Acta 545, 429–444
40 Clayton, R.K. and Wang, R.T. (1971) Methods Enzymol. 23, 696–704
41 Wraight, C.A. (1979) Biochim. Biophys. Acta 548, 309–327
42 Feher, G. and Okamura, (1978) in The Photosynthetic Bacteria (Clayton, R.A. and Sistrom, W.R., eds.), pp. 349–386, Plenum Press, New York
43 Snozzi, M. and Bachofen (1979) Biochim. Biophys. Acta 546, 236–247
44 Bevington, P.R. (1969) Data Reduction and Error Analysis for the Physical Sciences, McGraw-Hill, New York
45 Grinvald, A. (1976) Anal. Biochem. 75, 260–280
46 Rademaker, H., Hoff, A.J., Van Grondelle, R. and Duysens, L.N.M. (1980) Biochim. Biophys. Acta 592, 240–257
47 Prince, R.C., Tiede, D.M., Thornber, J.P. and Dutton, P.L. (1977) Biochim. Biophys. Acta 462, 467–490
48 Okamura, M.Y., Isaacson, R.A. and Feher, G. (1979) Biochim. Biophys. Acta 546, 394–417
49 Paschenko, V.Z., Kononenko, A.A., Protasov, S.P., Rubin, A.B., Rubin, L.B. and Uspenskaya, N.Ya. (1977) Biochim. Biophys. Acta 461, 403–412
50 Wraight, C.A. and Clayton, R.K. (1974) Biochim. Biophys. Acta 333, 246–260
51 Arata, H. and Parson, W.W. (1981) Biochim. Biophys. Acta 638, 201–209
52 Strickler, S.J. and Berg, R.A. (1962) J. Chem. Phys. 37, 814–822
53 Straley, S.C., Parson, W.W., Mauzerall, D.C. and Clayton, R.K. (1973) Biochim. Biophys. Acta 305, 597–609
54 Prince, R.C., Leigh. J.S. and Dutton, P.L. (1976) Biochim. Biophys. Acta 440, 622–636
55 Shuvalov, V.A., Krakhmaleva, I.N. and Klimov, V.V. (1976) Biochim. Biophys. Acta 449, 597–601
56 Rutherford, A.W., Heathcote, P. and Evans, M.C.W. (1979) Biochem. J. 182, 515–523
57 Clayton, R.K. (1978) Biochim. Biophys. Acta 504, 255–264